

**Supporting Information for**

**Lutetium(III) porphyrinoids as effective triplet photosensitizers for  
photon upconversion based on triplet-triplet annihilation (TTA)**

Zi-Shu Yang, Yingying Ning, Hao-Yan Yin and Jun-Long Zhang\*

Beijing National Laboratory for Molecular Sciences, State Key Laboratory of Rare Earth Materials  
Chemistry and Applications, College of Chemistry and Molecular Engineering, Peking University,  
Beijing 100871, P. R. China

Email: zhangjunlong@pku.edu.cn

## Contents

<b>Fig. S1-S4</b> $^1\text{H}$ NMR spectrum of <b>Lu-1-4</b> .....	3
<b>Fig. S5-S8</b> $^{19}\text{F}$ NMR spectrum of <b>Lu-1-4</b> .....	7
<b>Fig. S9-S12</b> $^{13}\text{C}$ NMR spectrum of <b>Lu-1-4</b> .....	11
<b>Fig. S13-S16</b> HR ESI-MS spectrum of <b>Lu-1-4</b> .....	15
<b>Fig. S17-S20</b> Normalized FT-IR spectrum of <b>Lu-1-4</b> .....	19
<b>Fig. S21</b> Normalized UV/Vis absorption spectra and emission spectra of <b>M-1</b> (M = Gd, Pd, Zn) in degassed toluene at room temperature.....	23
<b>Fig. S22-S27</b> Phosphorescence spectra and the Stern–Volmer plot of <b>M-1</b> (M = Gd, Pd, Zn) and <b>Lu-2-4</b> with BPEA in different concentration. ( $[\text{sensitizer}] = 0.5 \mu\text{M}$ , $\lambda_{\text{ex}} = 561 \text{ nm}$ ).....	24
<b>Fig. S28-S31</b> Upconverted fluorescence spectra of different TTA upconverted systems at different excitation power, and the double logarithmic plots of upconversion intensity as a function of incident power density in degassed toluene. ( $[\text{sensitizer}] = 0.5 \mu\text{M}$ ).....	30
<b>Fig. S32-S33</b> Decay spectra of the delayed fluorescence boserved in TTA upconversion systems with <b>Lu-2-4</b> and <b>M-1</b> (M = Gd, Pd, Zn) as sensitizers and BPEA or rubrene as acceptor in degassed toluene. ....	34
<b>Fig. S34</b> Upconversion efficiencies ( $\Phi_{\text{UC}}$ ) as a function of BPEA concentration with the sensitizer at fixed concentration ( $0.5 \mu\text{M}$ ) in degassed toluene. ( $\lambda_{\text{ex}} = 561 \text{ nm}$ , $480 \text{ mW}\cdot\text{cm}^{-2}$ ).....	36
<b>Fig. S35</b> Stability of the TTA upconversion emission of different upconversion systems upon continuous irradiation in degassed toluene. ( $480 \text{ mW}\cdot\text{cm}^{-2}$ ).....	37
<b>Fig. S36</b> TEM image and size distribution of UC-NMs loaded with <b>Lu-2/BPEA</b> .....	38
<b>Fig. S37</b> Size distribution of UC-MSNs loaded with <b>Lu-1/BPEA</b> .....	39
<b>Fig. S38</b> TEM image and size distribution of UC-MSNs loaded with <b>Lu-2/BPEA</b> .....	40
<b>Fig. S39-S40</b> DLS curve of UC-NMs and UC-MSNs loaded with <b>Lu-2/BPEA</b> .....	41
<b>Fig. S41-S42</b> Normalized absorption and emission spectra of UC-NMs and UC-MSNs loaded with <b>Lu-2/BPEA</b> pair in water under ambient atmosphere.....	43
<b>Fig. S43</b> Confocal fluorescence image of living HeLa cell with UC-NMs and UC-MSNs loaded with BPEA only.....	45

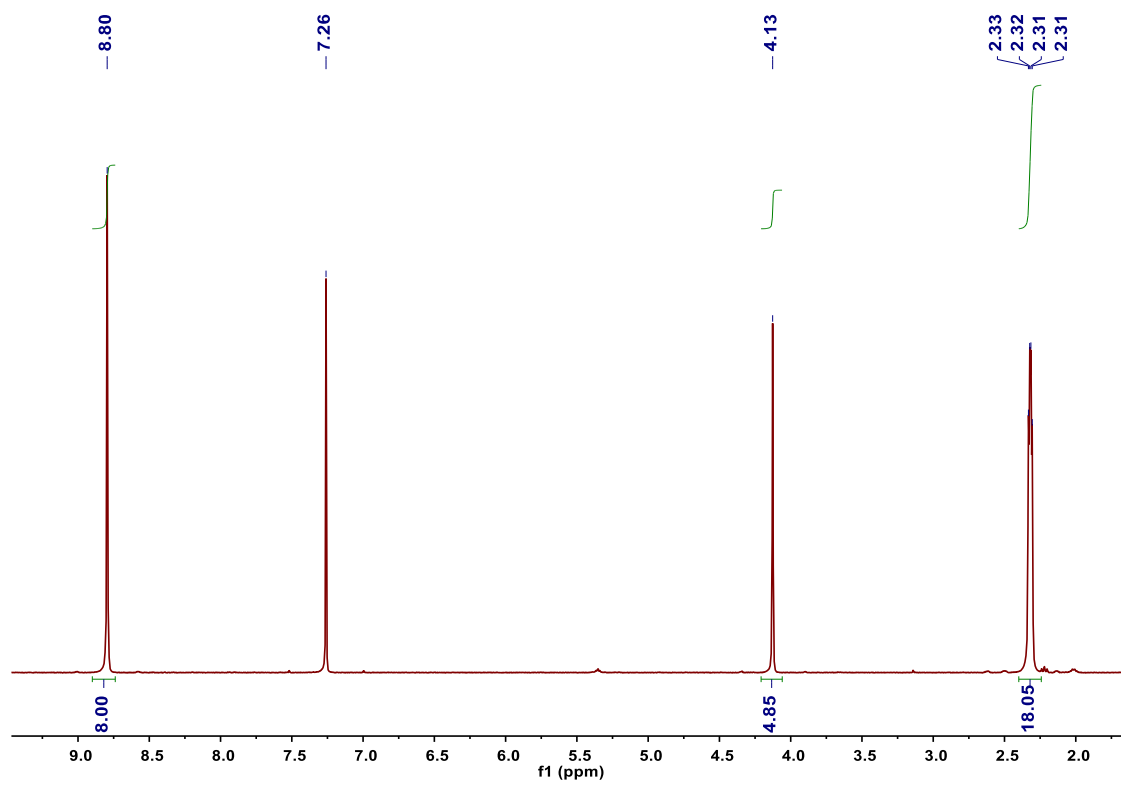


**Fig. S1** <sup>1</sup>H NMR spectrum of **Lu-1** (400 MHz, CDCl<sub>3</sub>).

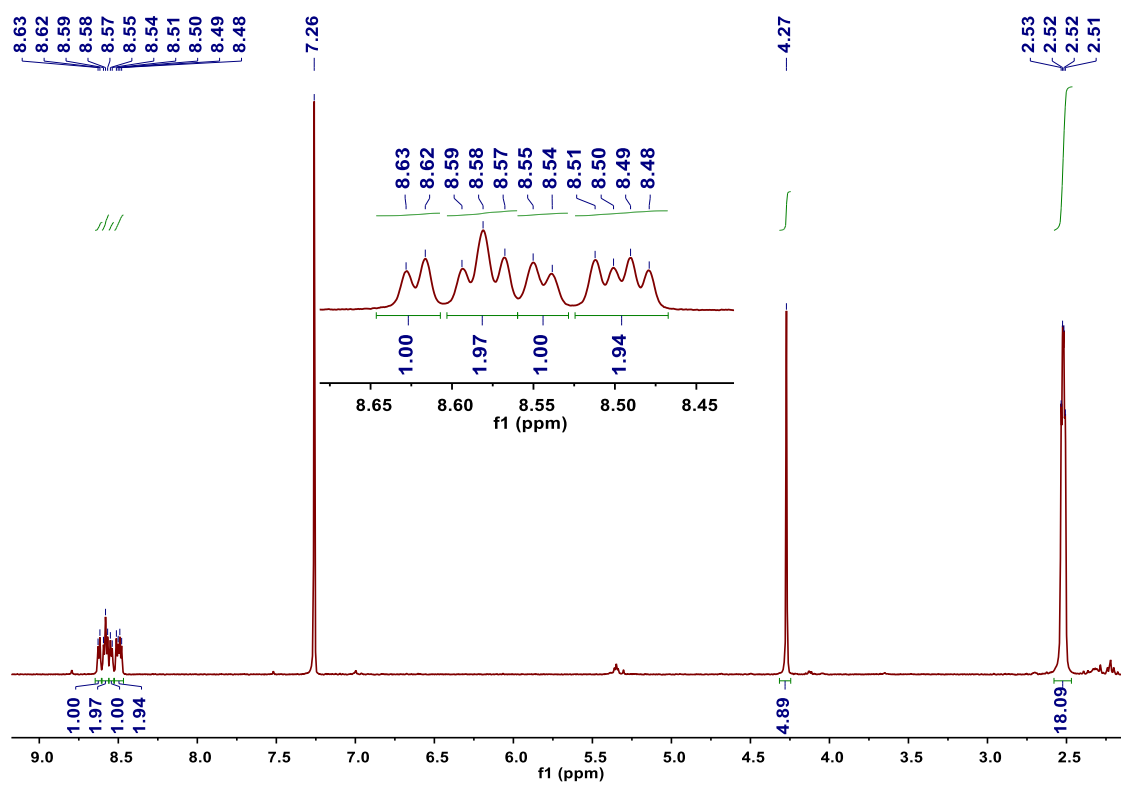


Fig. S2  $^1\text{H}$  NMR spectrum of Lu-2 (400 MHz,  $\text{CDCl}_3$ ).

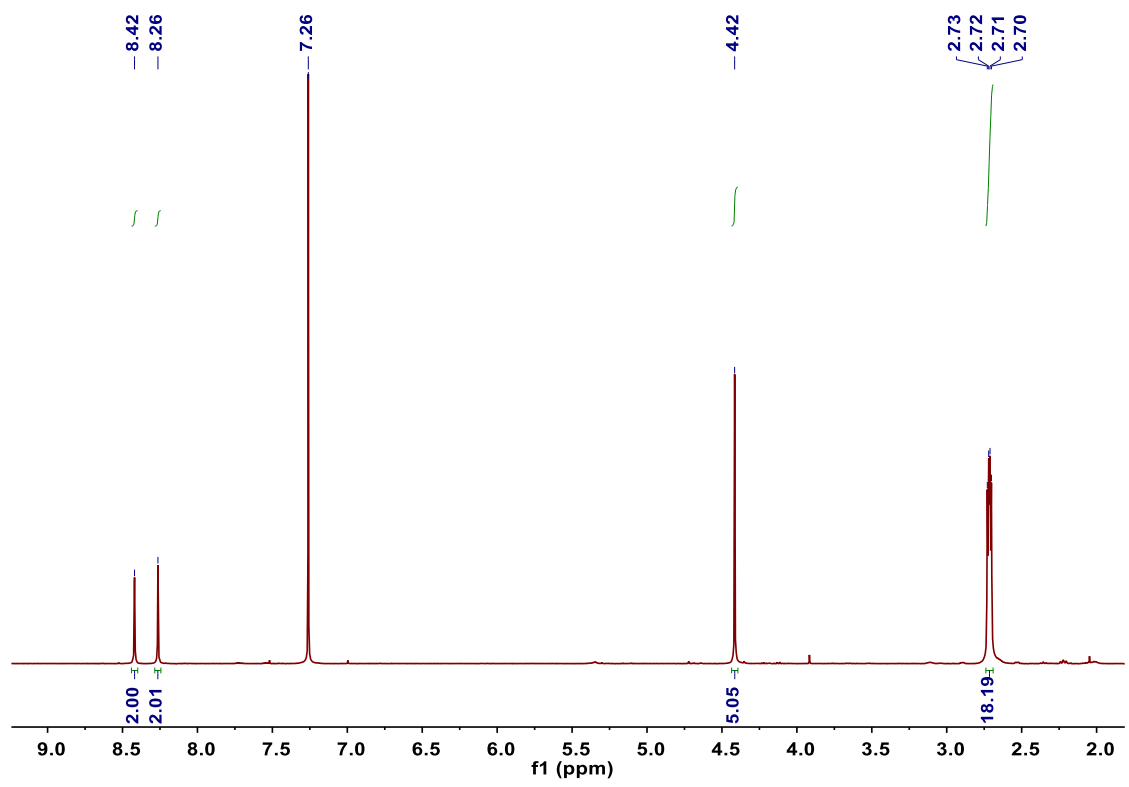


Fig. S3 <sup>1</sup>H NMR spectrum of Lu-3 (400 MHz, CDCl<sub>3</sub>).

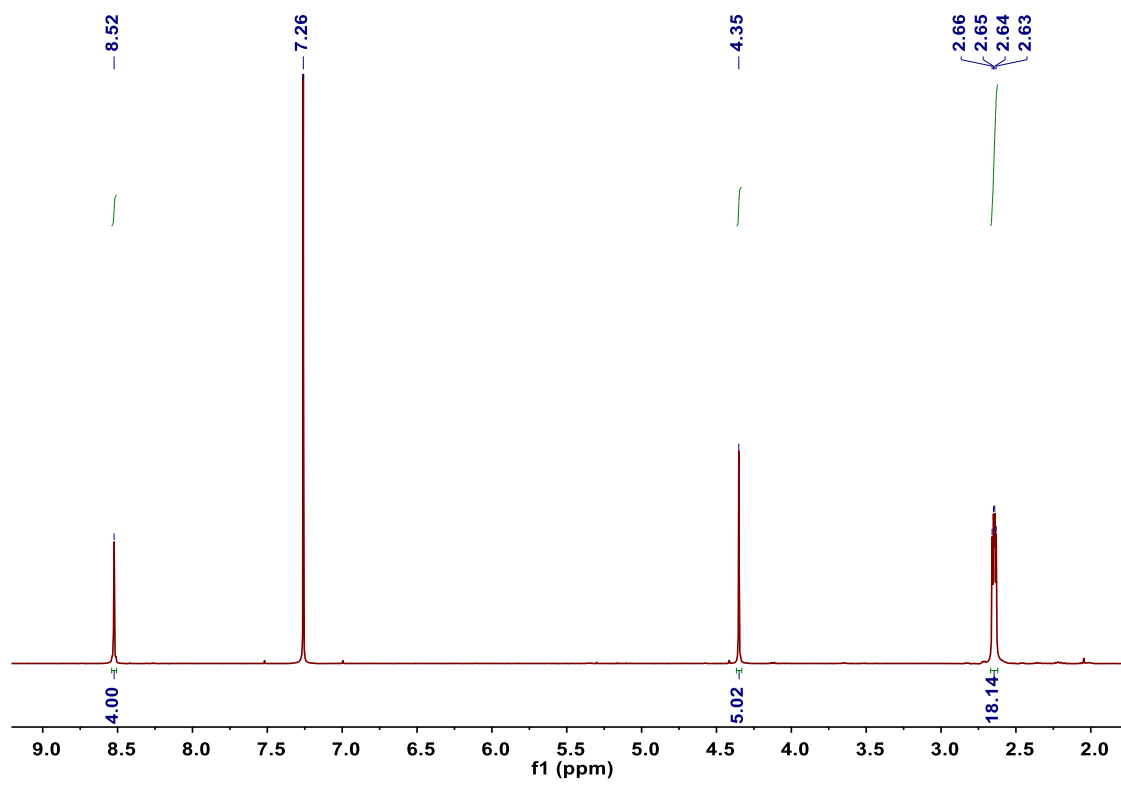


Fig. S4 <sup>1</sup>H NMR spectrum of Lu-4 (400 MHz, CDCl<sub>3</sub>).

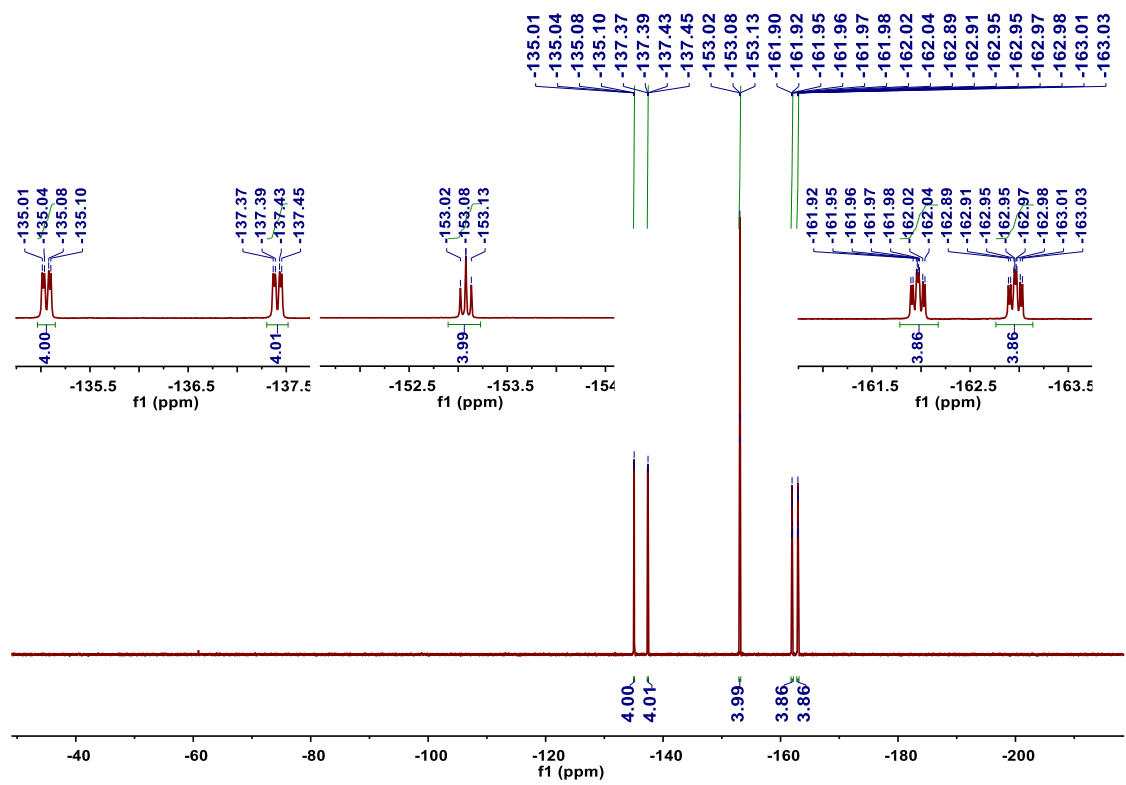


Fig. S5  $^{19}\text{F}$  NMR spectrum of Lu-1 (377 MHz,  $\text{CDCl}_3$ ).



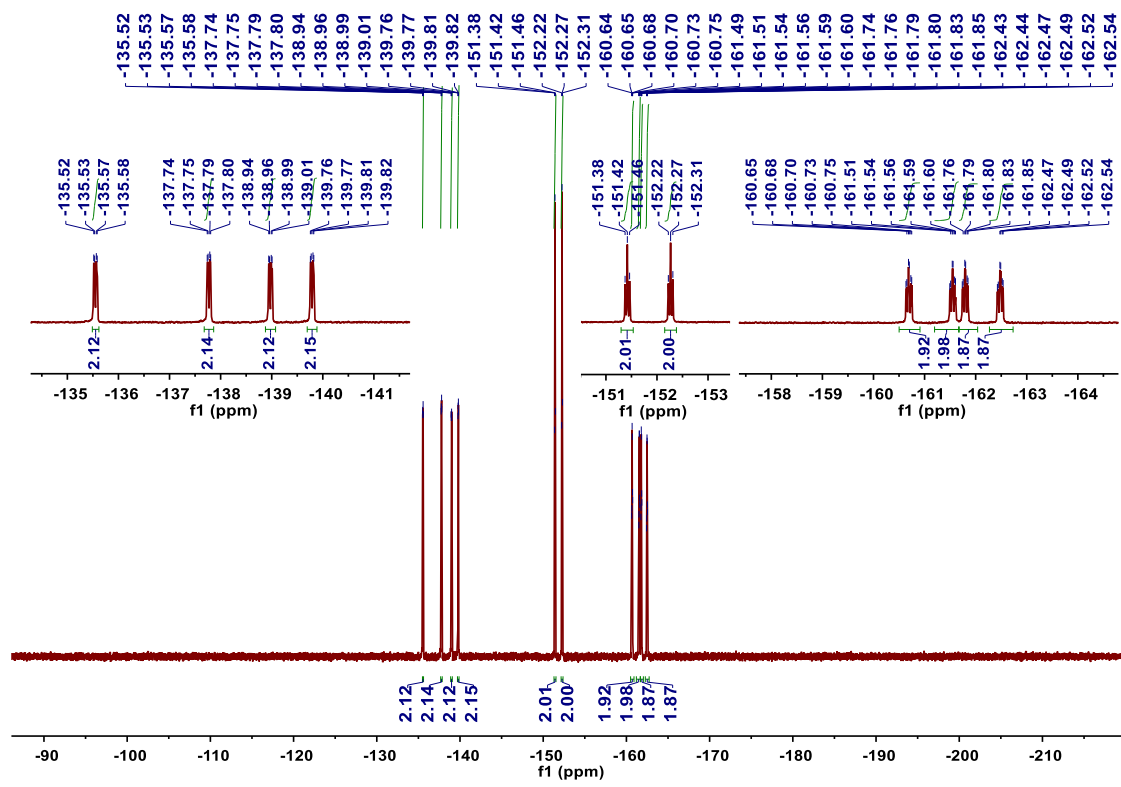


Fig. S7  $^{19}\text{F}$  NMR spectrum of Lu-3 (471 MHz,  $\text{CDCl}_3$ ).

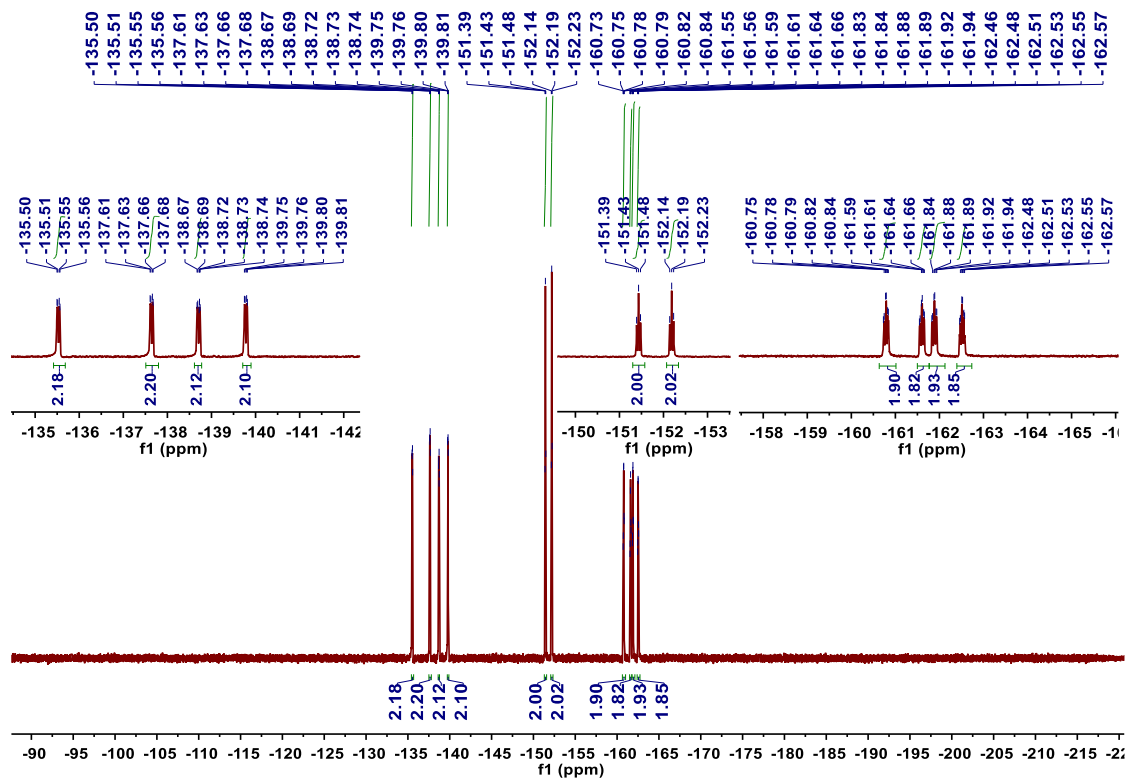


Fig. S8  $^{19}\text{F}$  NMR spectrum of Lu-4 (471 MHz,  $\text{CDCl}_3$ ).

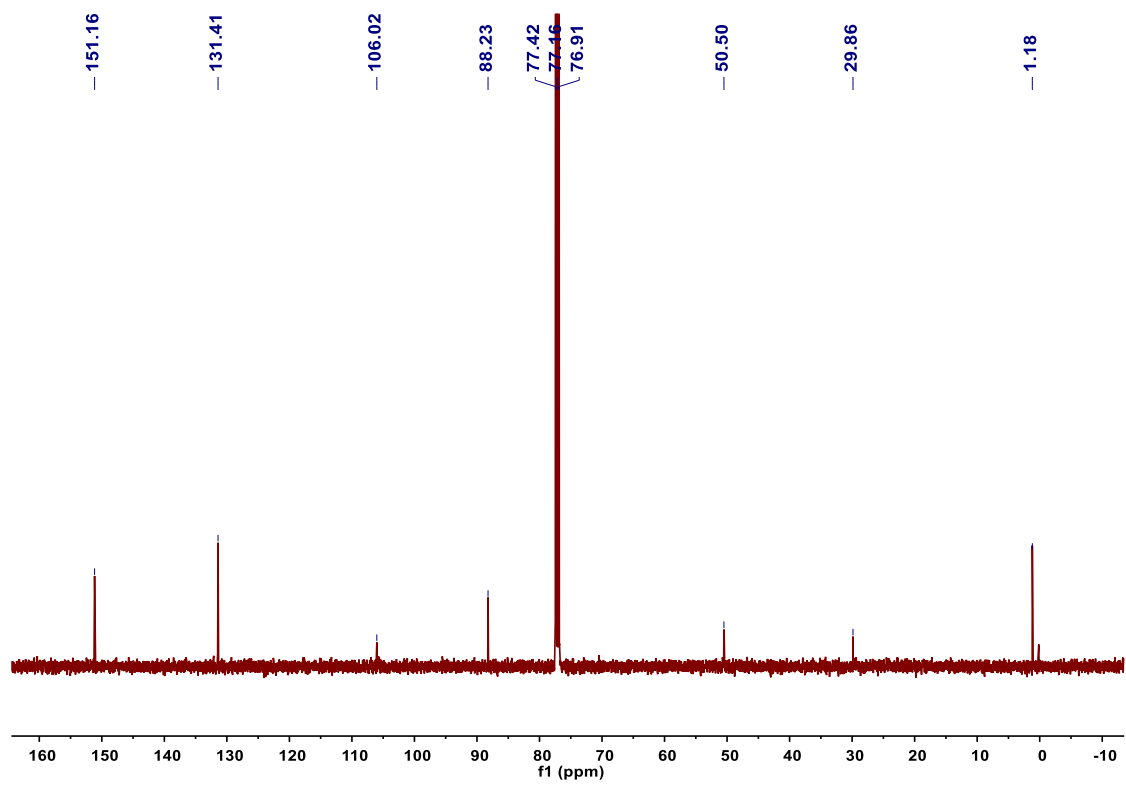


Fig. S9  $^{13}\text{C}$  NMR spectrum of Lu-1 (126 MHz,  $\text{CDCl}_3$ ).

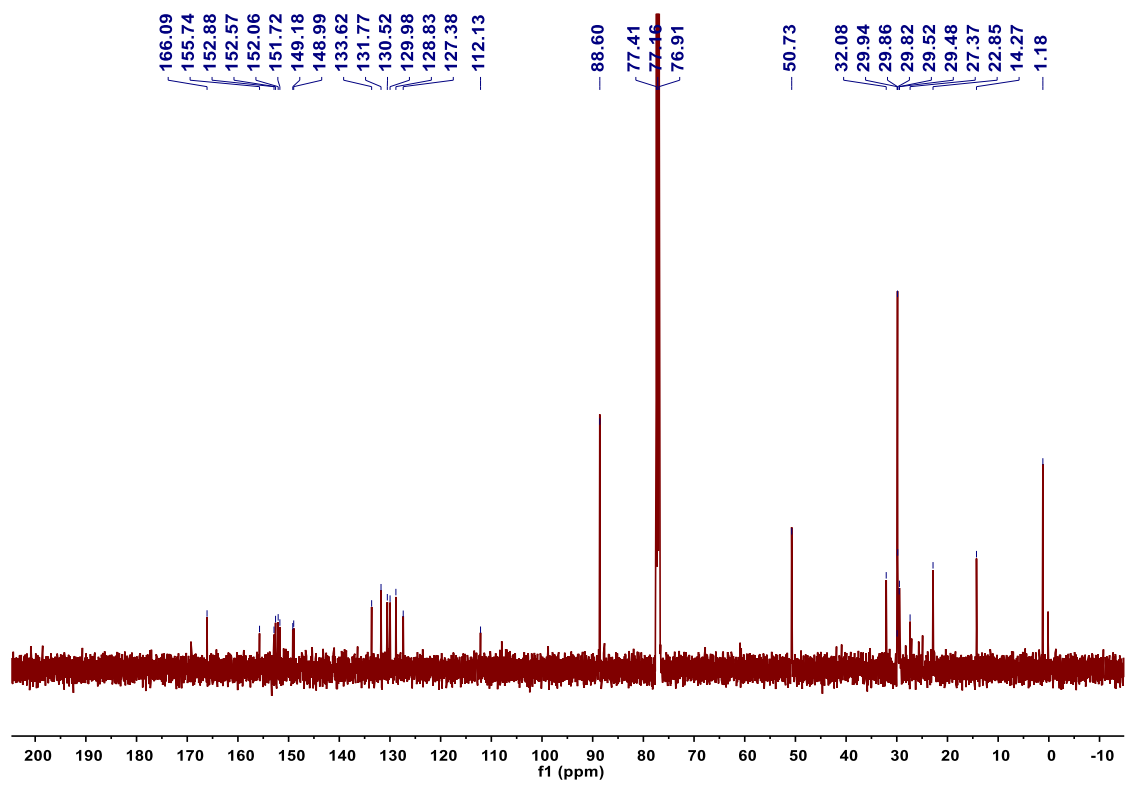


Fig. S10 <sup>13</sup>C NMR spectrum of Lu-2 (126 MHz, CDCl<sub>3</sub>).

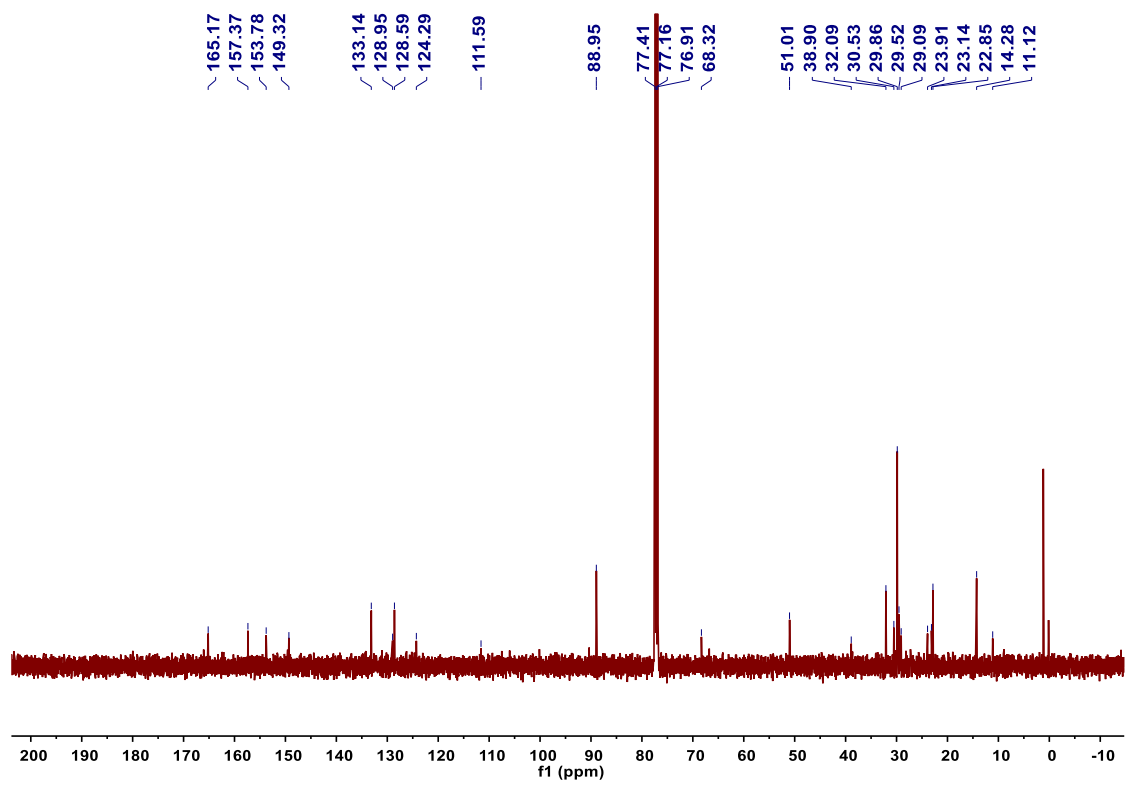


Fig. S11 <sup>13</sup>C NMR spectrum of Lu-3 (126 MHz, CDCl<sub>3</sub>).

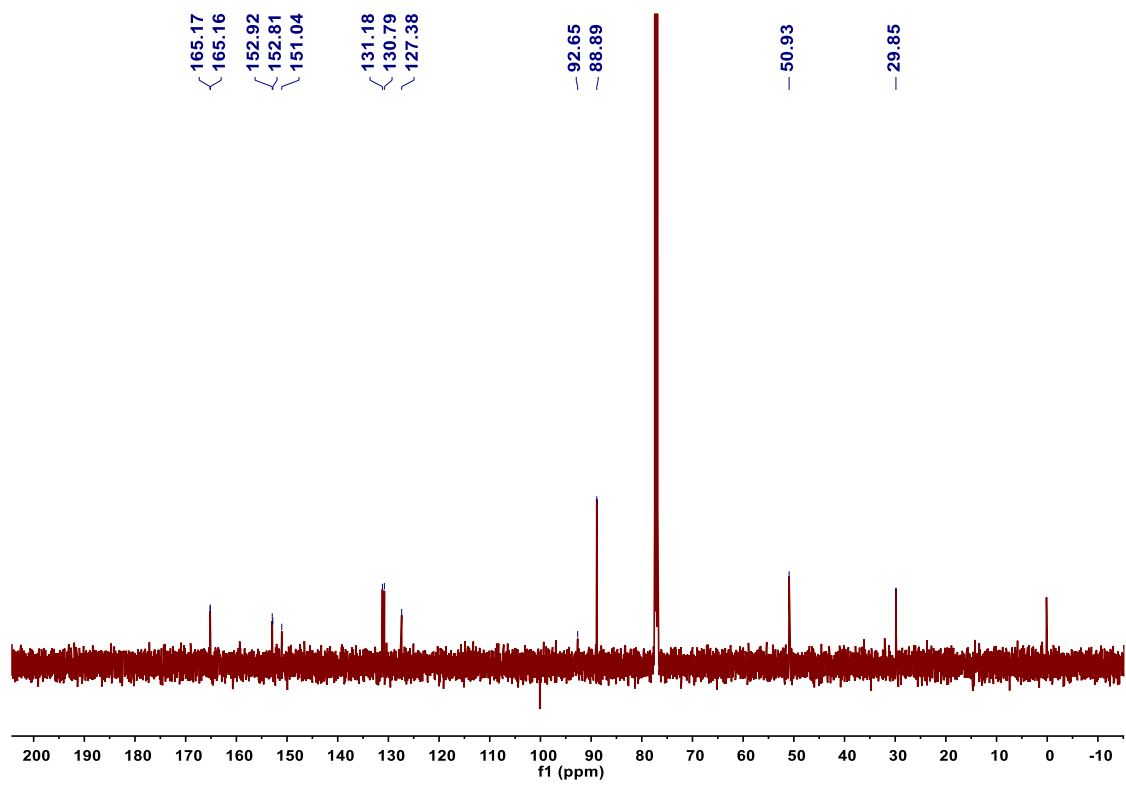


Fig. S12  $^{13}\text{C}$  NMR spectrum of Lu-4 (126 MHz,  $\text{CDCl}_3$ ).

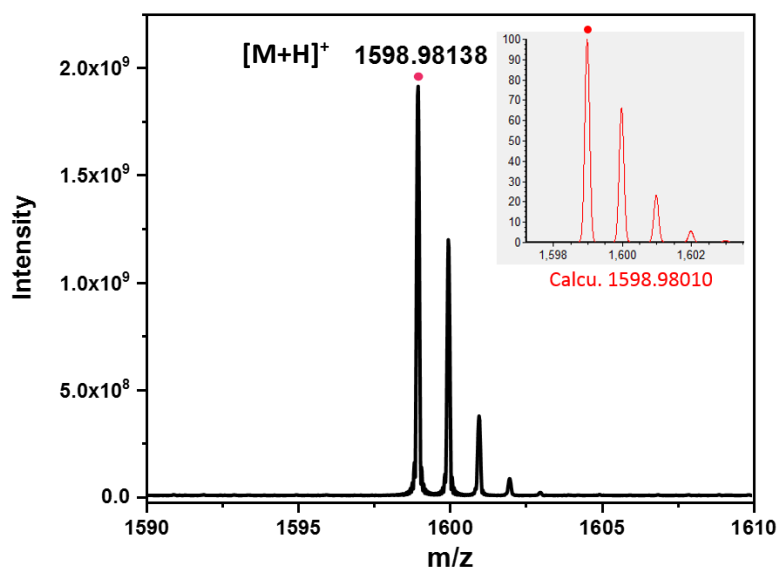


Fig. S13 HR ESI-MS spectrum of Lu-1. Inset presents the simulated spectrum.

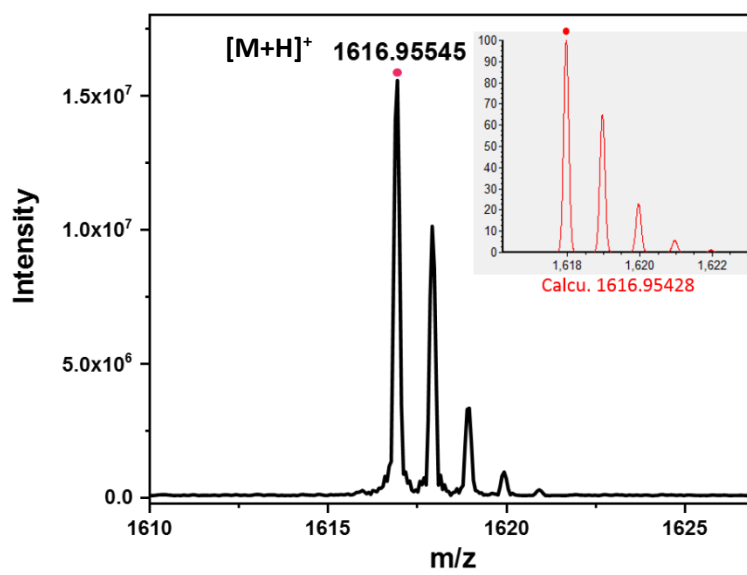


Fig. S14 HR ESI-MS spectrum of Lu-2. Inset presents the simulated spectrum.

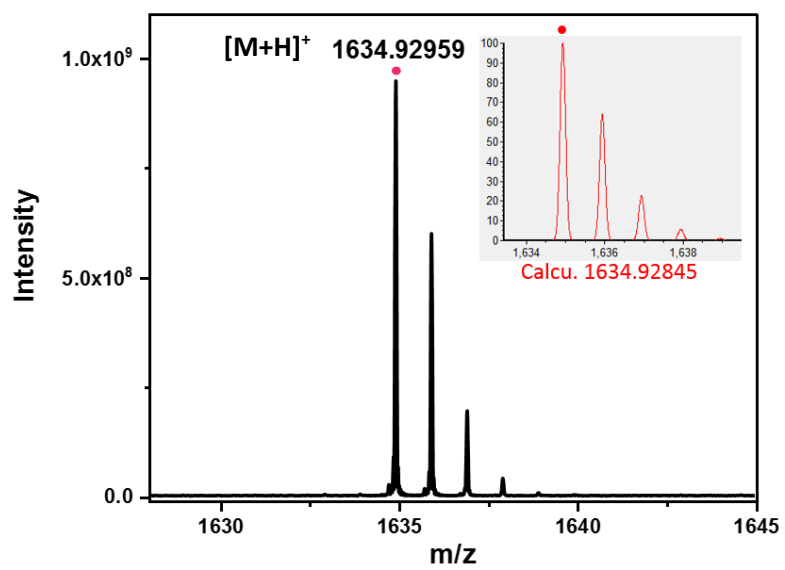


Fig. S15 HR ESI-MS spectrum of Lu-3. Inset presents the simulated spectrum.

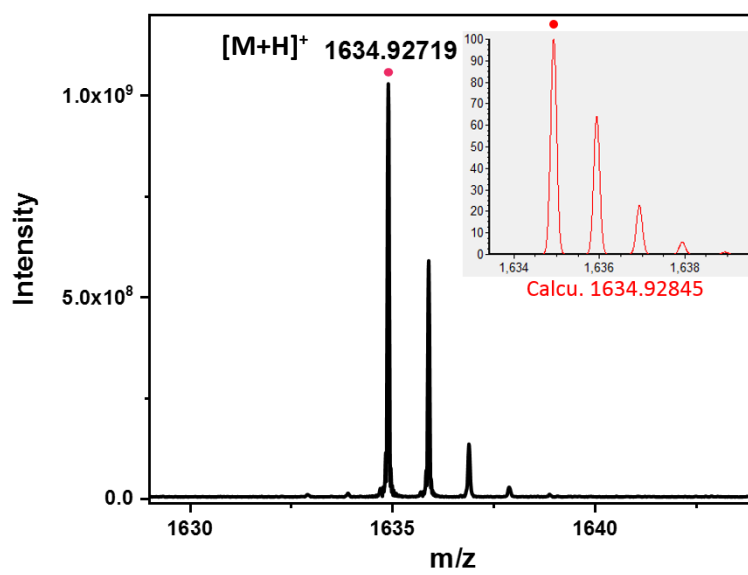
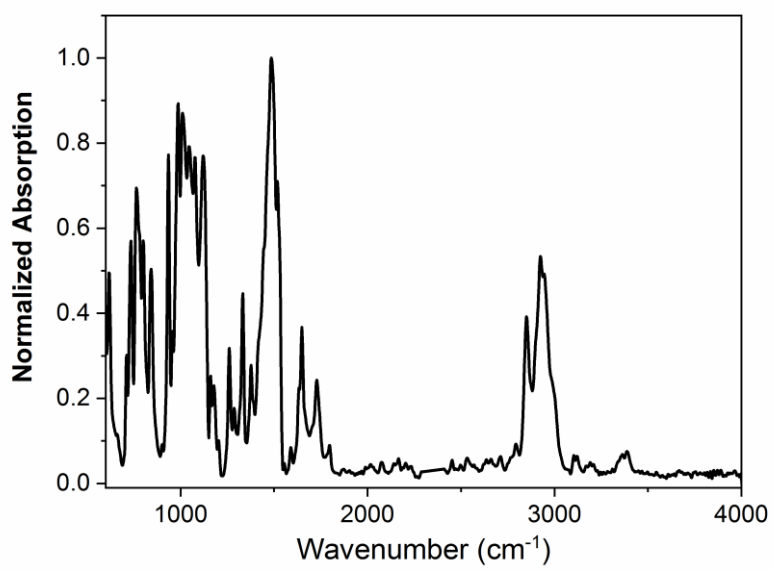


Fig. S16 HR ESI-MS spectrum of Lu-4. Inset presents the simulated spectrum.



**Fig. S17** Normalized FT-IR spectrum of **Lu-1**.

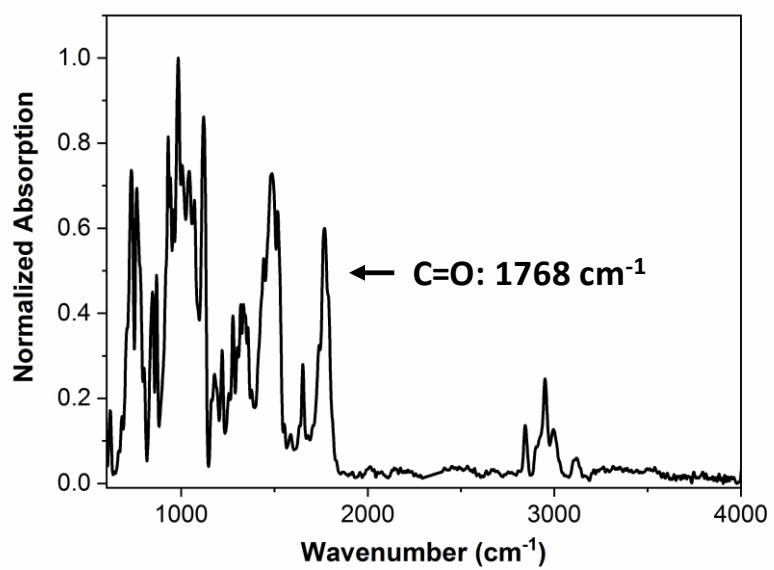


Fig. S18 Normalized FT-IR spectrum of Lu-2.

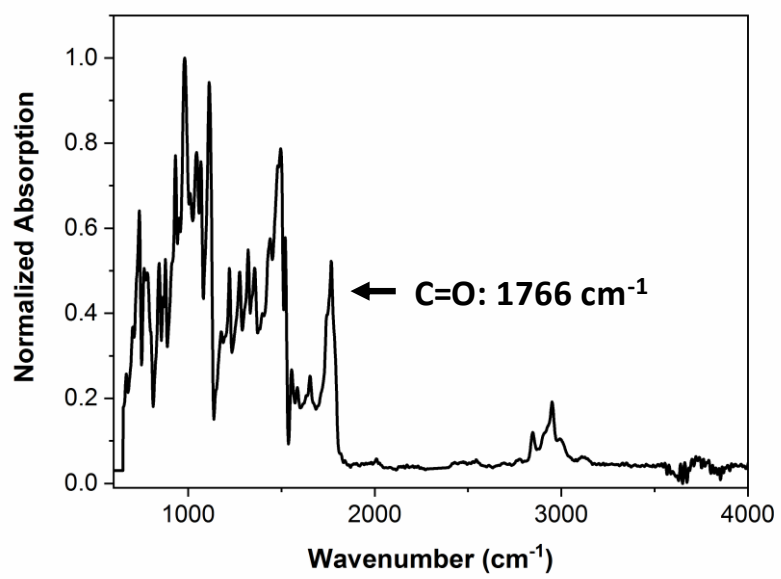
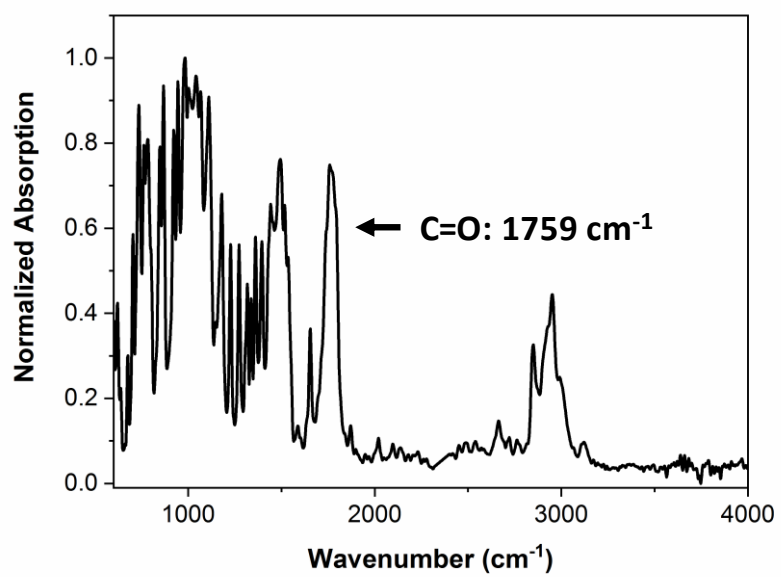
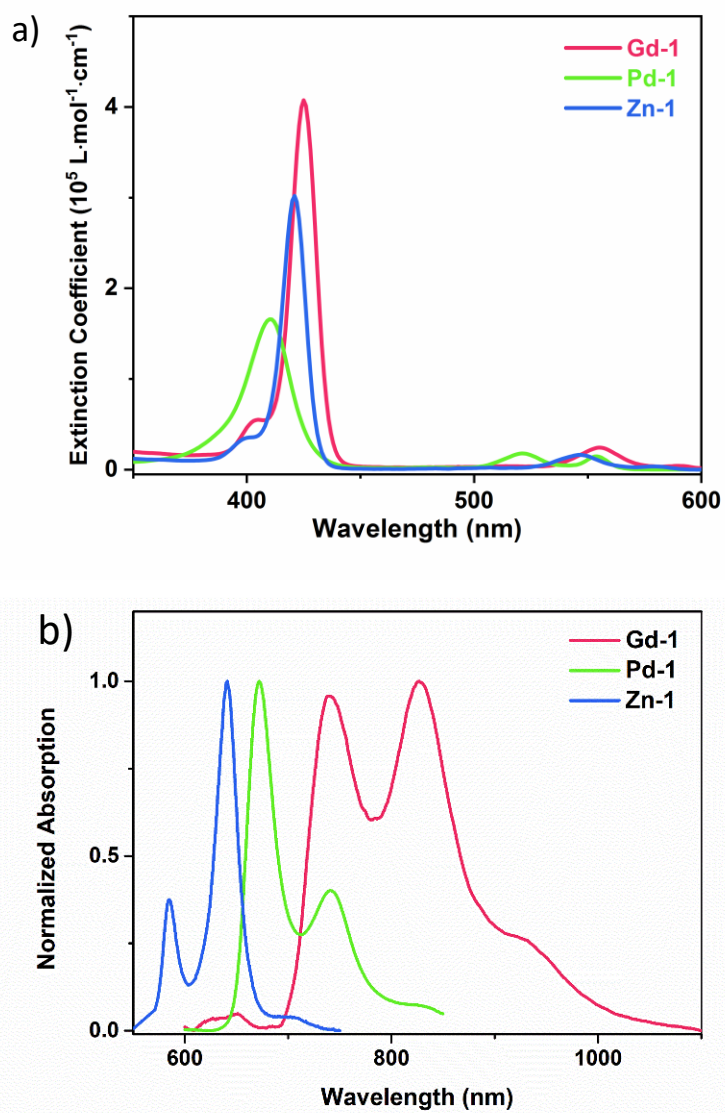


Fig. S19 Normalized FT-IR spectrum of Lu-3.



**Fig. S20** Normalized FT-IR spectrum of **Lu-4**.



**Fig. S21** (a) UV/Vis absorption spectra and (b) normalized emission spectra (excited at Soret bands) of **M-1** (M = Gd, Pd, Zn) in degassed toluene at room temperature.

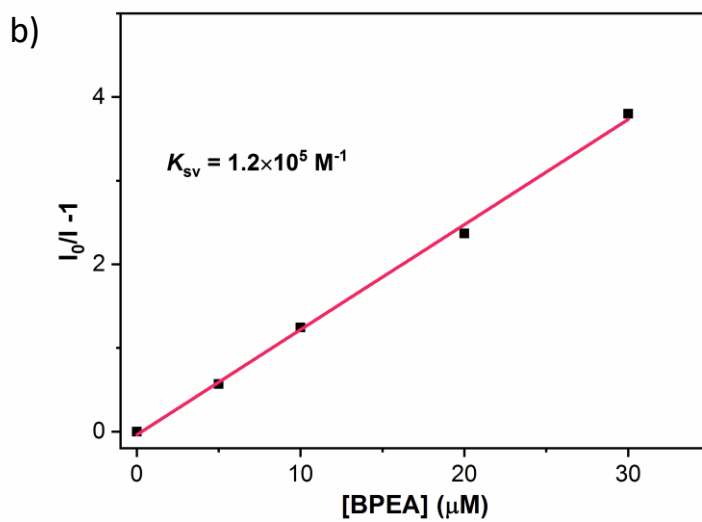
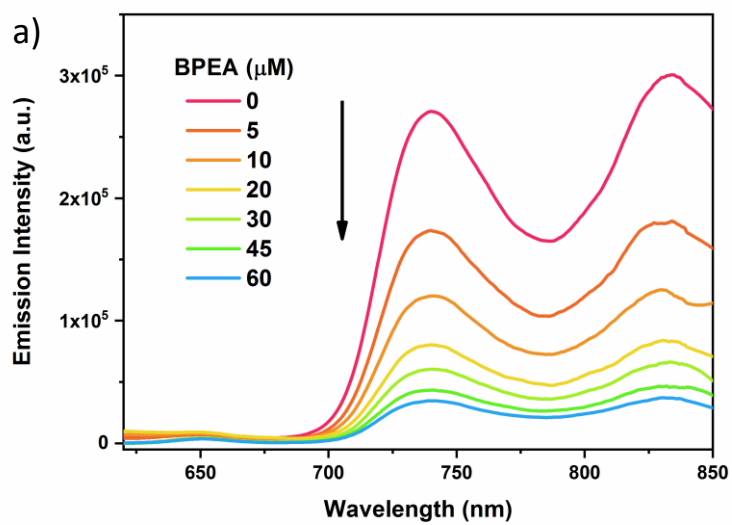


**Fig. S22** a) The phosphorescence spectra of **Gd-1** with BPEA in different concentration in degassed toluene; b) the Stern–Volmer plot of **Gd-1** with BPEA in degassed toluene. ( $[\text{Gd-1}] = 0.5 \mu\text{M}$ ,  $\lambda_{\text{ex}} = 561 \text{ nm}$ )

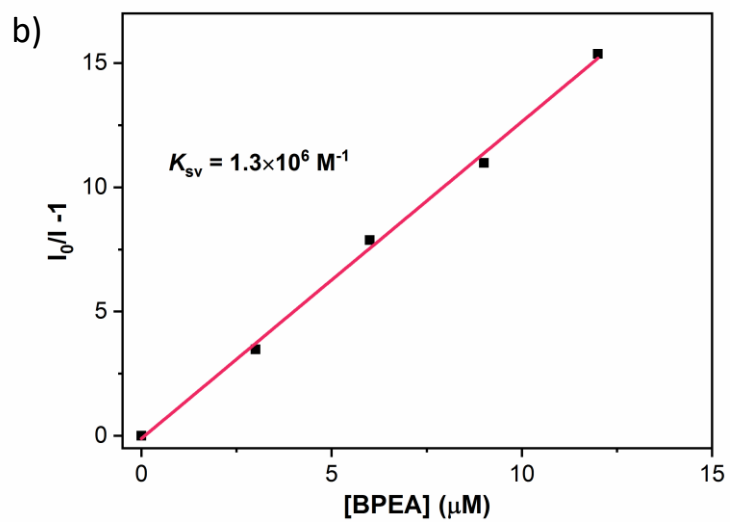
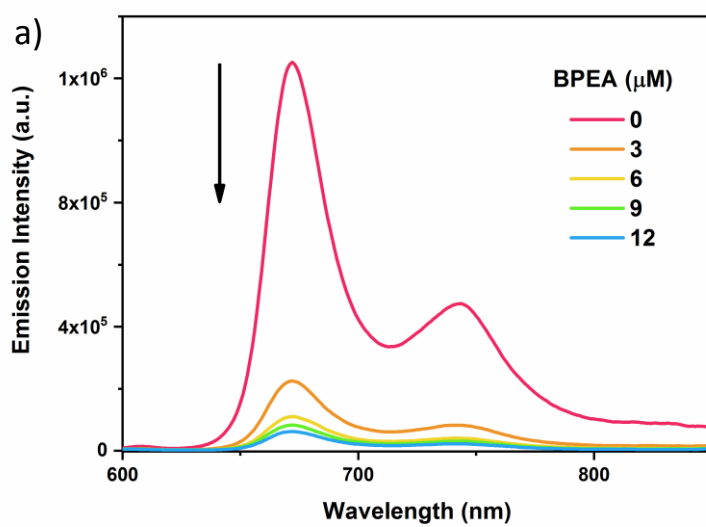


**Fig. S23** a) The phosphorescence spectra of **Pd-1** with BPEA in different concentration in degassed toluene; b) the Stern–Volmer plot of **Pd-1** with BPEA in degassed toluene. ( $[\text{Pd-1}] = 0.5 \mu\text{M}$ ,  $\lambda_{\text{ex}} = 561 \text{ nm}$ )

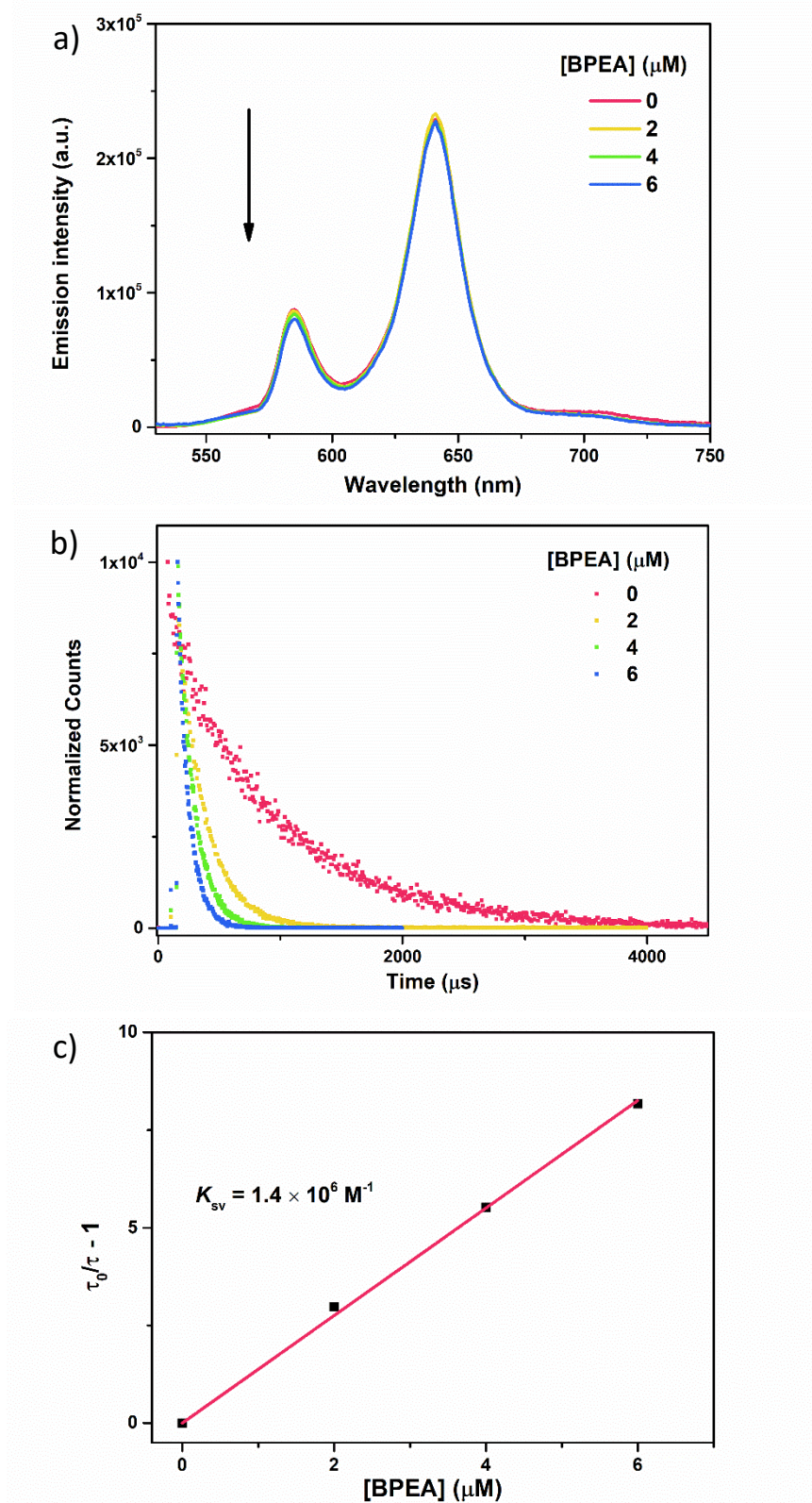


**Fig. S24** a) The emission and b) decay ( $\lambda_{\text{em}} = 715 \text{ nm}$ ) spectra of **Zn-1** with BPEA in different concentration in degassed toluene; c) the Stern–Volmer plot of **Zn-1** with BPEA in degassed toluene ( $K_{\text{sv}}$  is determined according to  $\tau_0/\tau = 1 + K_{\text{sv}}[\text{BPEA}]$ , due to the weak phosphorescence of **Zn-1**). ( $[\text{Zn-1}] = 0.5 \mu\text{M}$ ,  $\lambda_{\text{ex}} = 561 \text{ nm}$ )

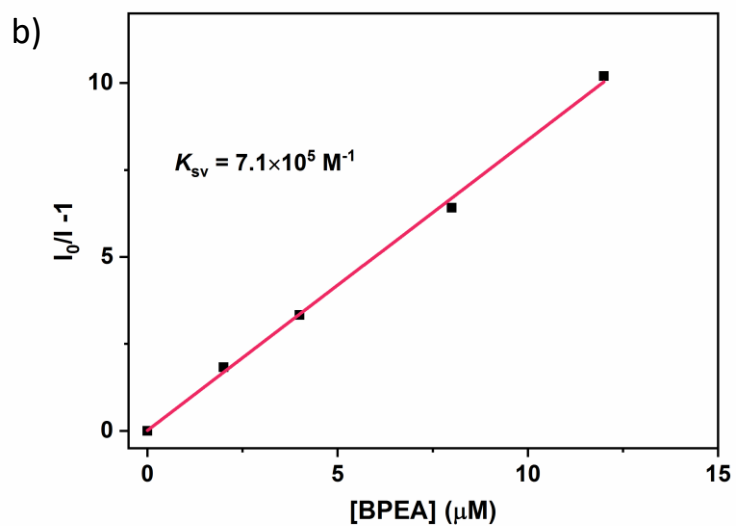
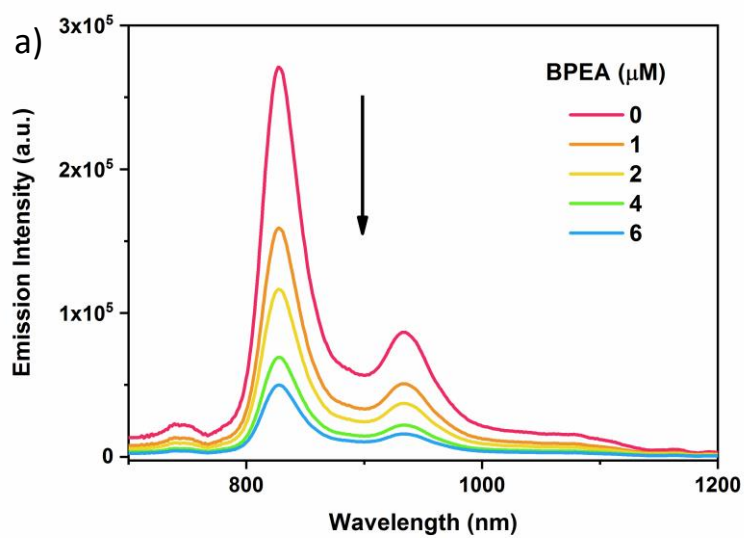


**Fig. S25** a) The phosphorescence spectra of Lu-2 with BPEA in different concentration in degassed toluene; b) the Stern–Volmer plot of Lu-2 with BPEA in degassed toluene. ( $[\text{Lu-2}] = 0.5 \mu\text{M}$ ,  $\lambda_{\text{ex}} = 561 \text{ nm}$ )

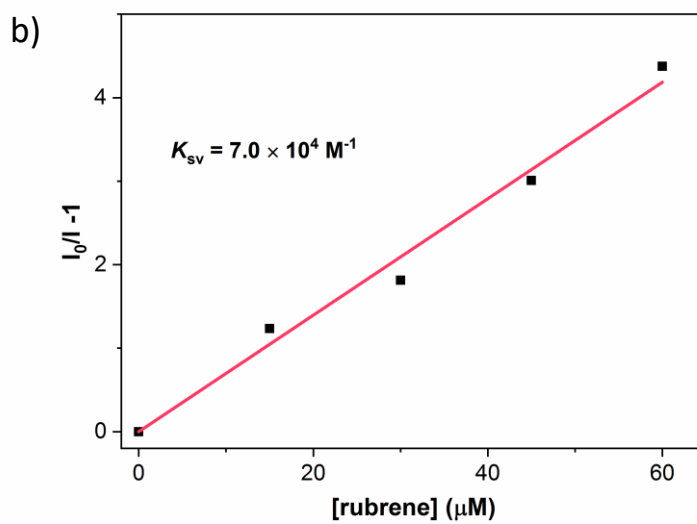
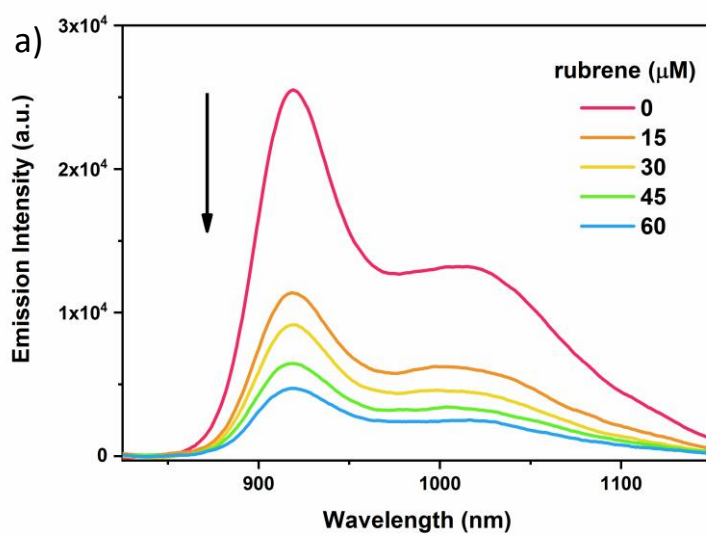


**Fig. S26** a) The phosphorescence spectra of **Lu-3** with rubrene in different concentration in degassed toluene; b) the Stern–Volmer plot of **Lu-3** with rubrene in degassed toluene. ( $[\text{Lu-3}] = 0.5 \mu\text{M}$ ,  $\lambda_{\text{ex}} = 639 \text{ nm}$ )

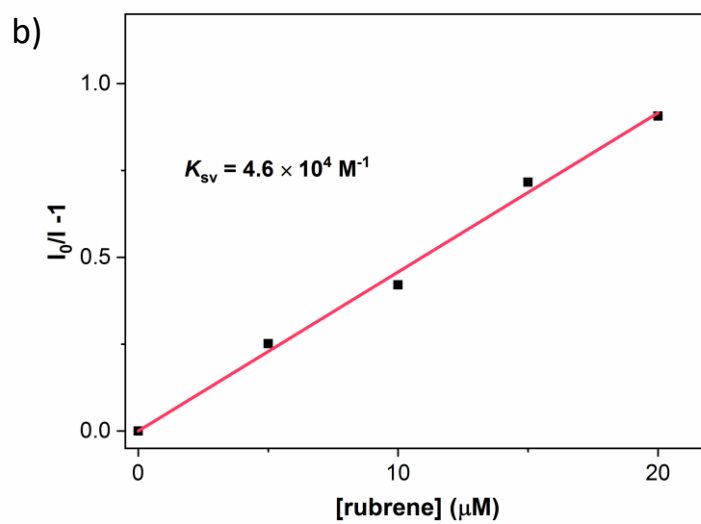
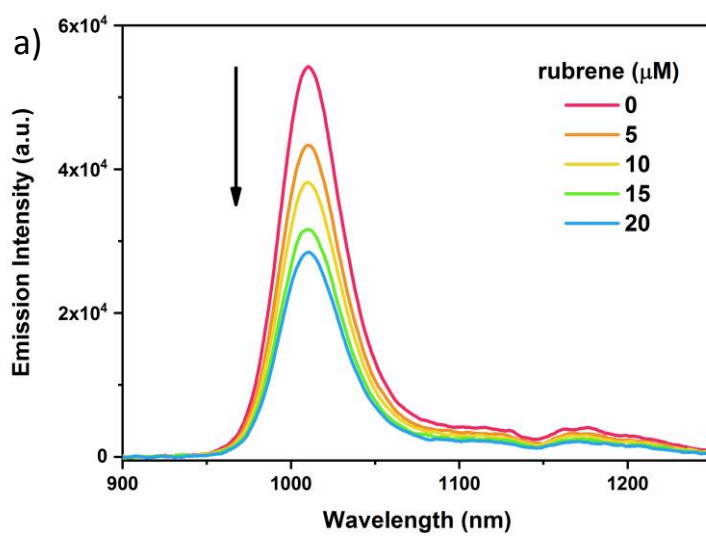


**Fig. S27** a) The phosphorescence spectra of **Lu-4** with rubrene in different concentration in degassed toluene; b) the Stern–Volmer plot of **Lu-4** with rubrene in degassed toluene. ( $[\text{Lu-4}] = 0.5 \mu\text{M}$ ,  $\lambda_{\text{ex}} = 659 \text{ nm}$ )

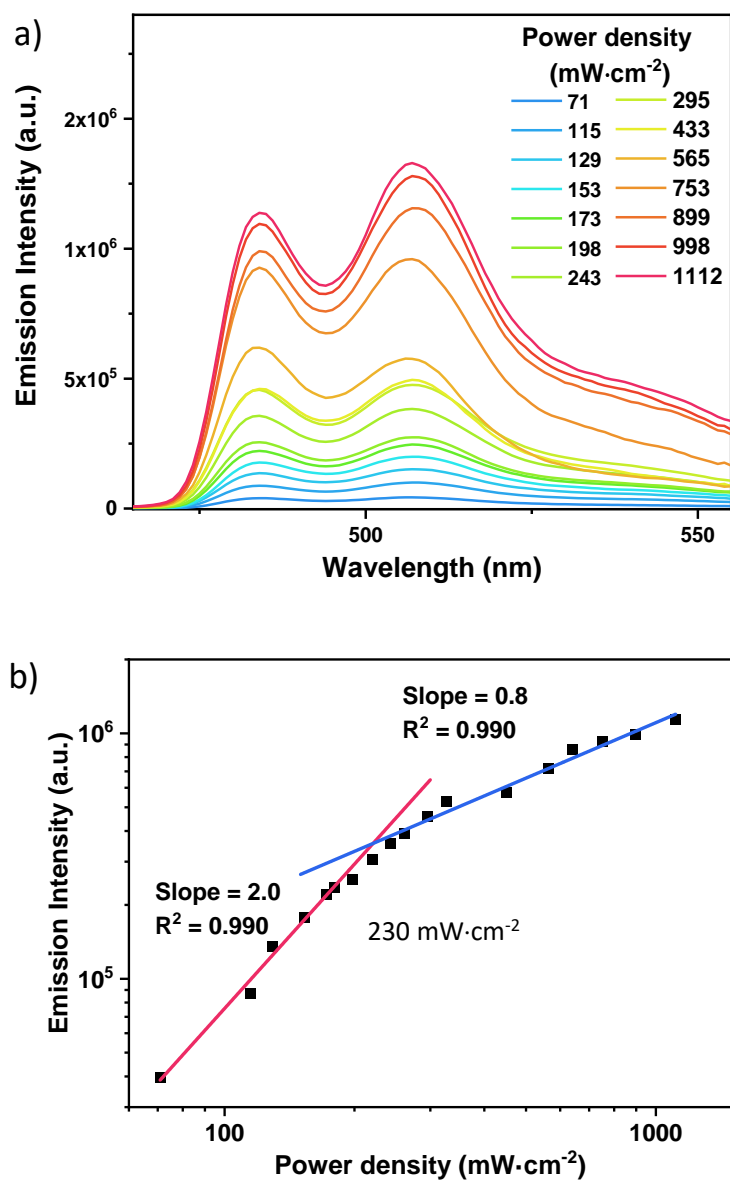


**Fig. S28** a) Upconverted fluorescence spectra of **Gd-1/BPEA** at different excitation power; b) the double logarithmic plots of upconversion intensity at 480 nm measured as a function of power density of a 561 nm incident laser for **Gd-1/BPEA** in degassed toluene (the threshold excitation power density = 230  $\text{mW}\cdot\text{cm}^{-2}$ ). ( $[\text{Gd-1}] = 0.5 \mu\text{M}$ ,  $[\text{BPEA}] = 60 \mu\text{M}$ ,  $\lambda_{\text{ex}} = 561 \text{ nm}$ )

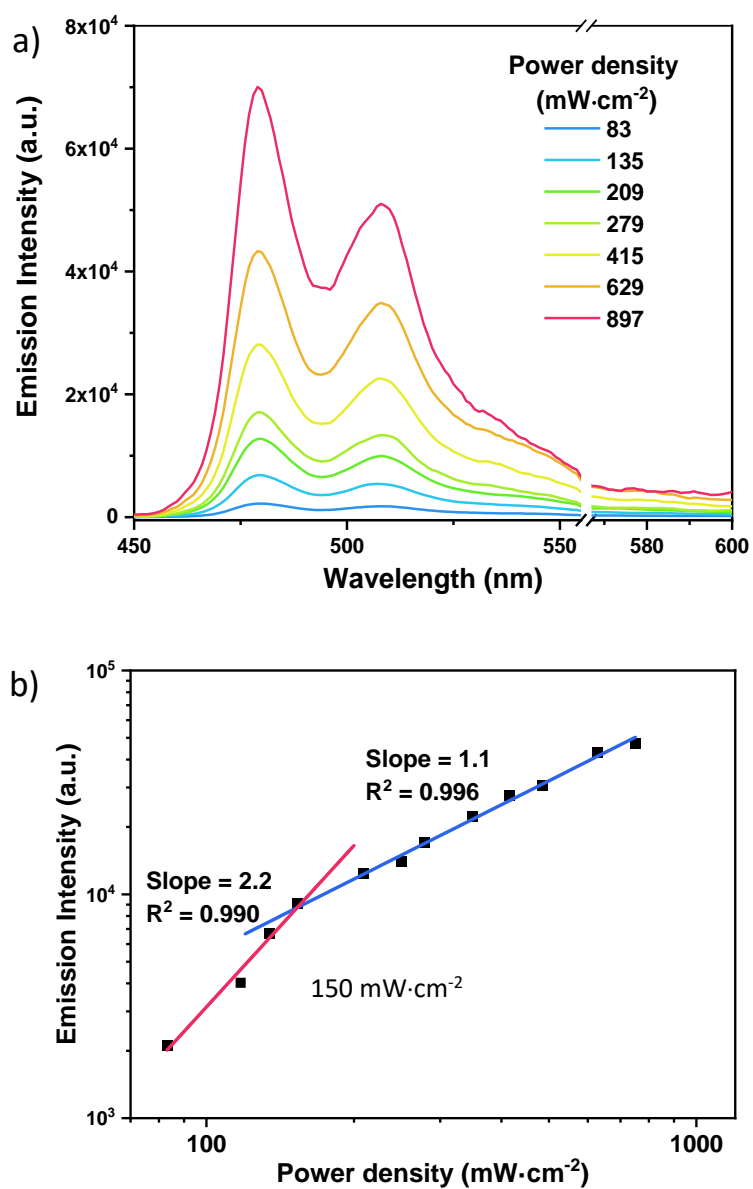


**Fig. S29** a) Upconverted fluorescence spectra of **Pd-1**/BPEA at different excitation power; b) the double logarithmic plots of upconversion intensity at 480 nm measured as a function of power density of a 561 nm incident laser for **Pd-1**/BPEA in degassed toluene (the threshold excitation power density =  $150 \text{ mW}\cdot\text{cm}^{-2}$ ). ( $[\text{Pd-1}] = 0.5 \mu\text{M}$ ,  $[\text{BPEA}] = 60 \mu\text{M}$ ,  $\lambda_{\text{ex}} = 561 \text{ nm}$ )

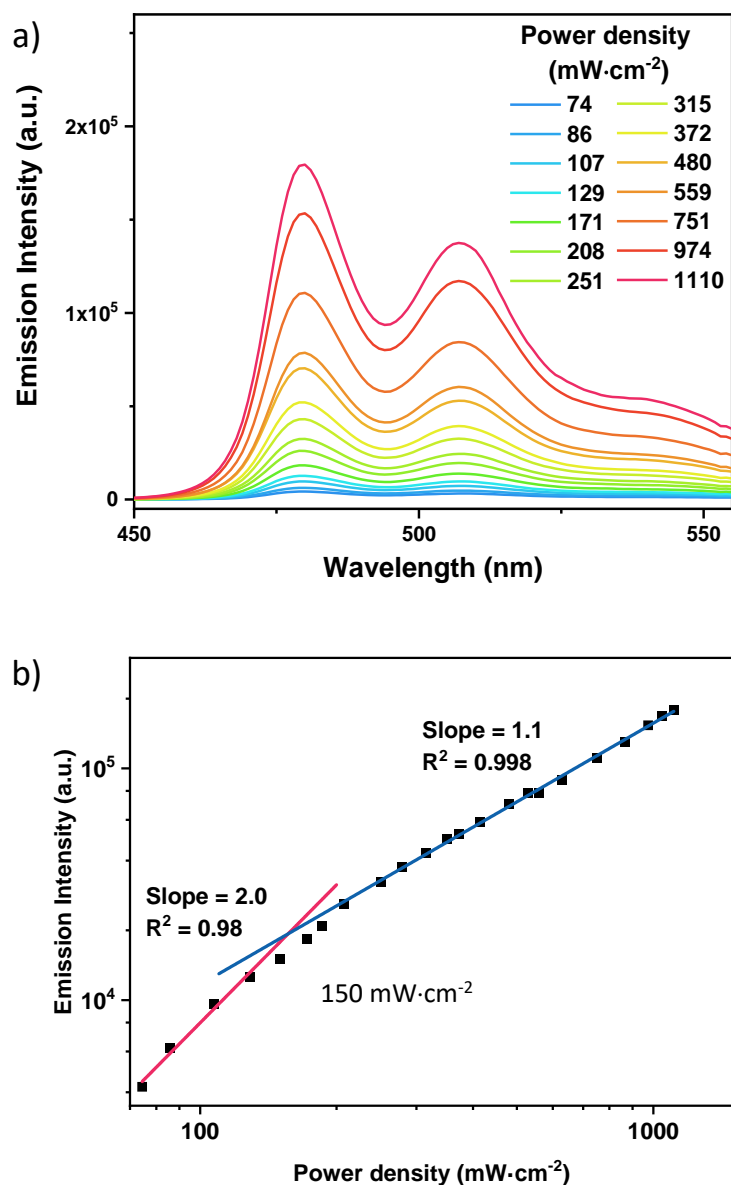


**Fig. S30** a) Upconverted fluorescence spectra of **Zn-1**/BPEA at different excitation power; b) the double logarithmic plots of upconversion intensity at 480 nm measured as a function of power density of a 561 nm incident laser for **Zn-1**/BPEA in degassed toluene (the threshold excitation power density = 150 mW·cm<sup>-2</sup>). ( $[\text{Zn-1}] = 0.5 \mu\text{M}$ ,  $[\text{BPEA}] = 60 \mu\text{M}$ ,  $\lambda_{\text{ex}} = 561 \text{ nm}$ )

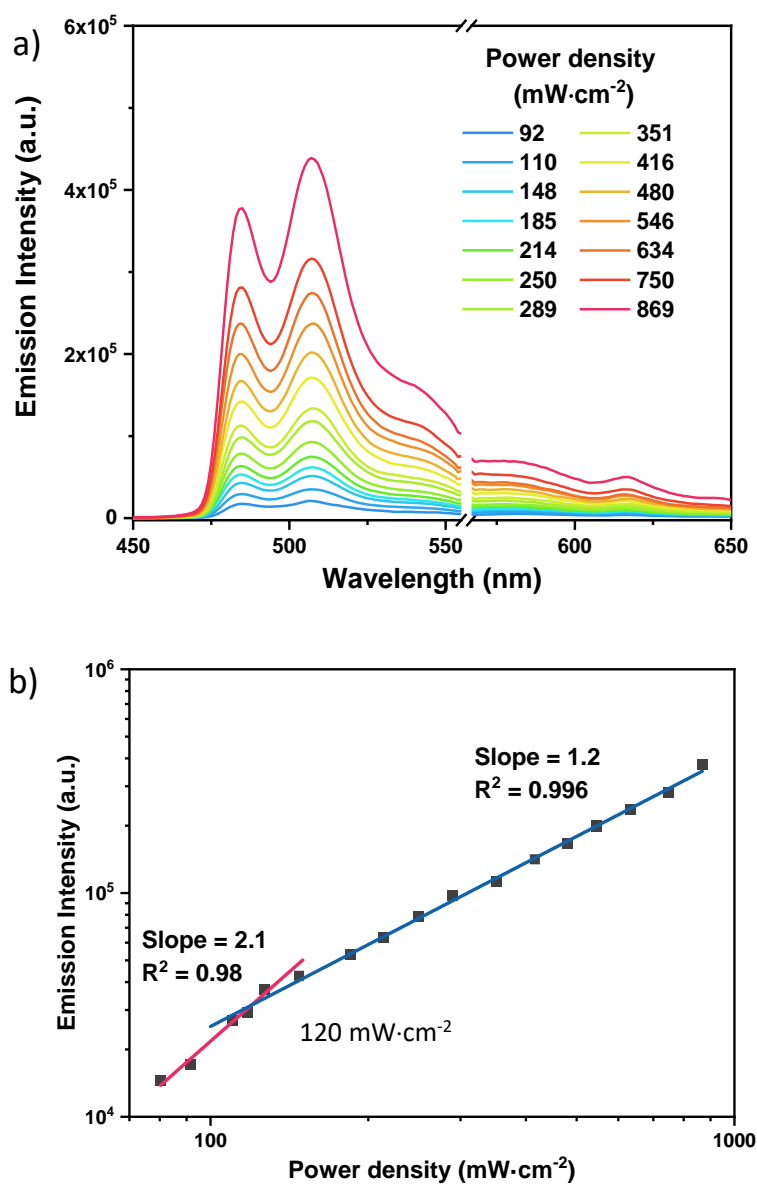


**Fig. S31** a) Upconverted fluorescence spectra of **Lu-2**/BPEA at different excitation power; b) the double logarithmic plots of upconversion intensity at 480 nm measured as a function of power density of a 561 nm incident laser for **Lu-2**/BPEA in degassed toluene (the threshold excitation power density =  $120 \text{ mW}\cdot\text{cm}^{-2}$ ). ( $[\text{Lu-2}] = 0.5 \mu\text{M}$ ,  $[\text{BPEA}] = 60 \mu\text{M}$ ,  $\lambda_{\text{ex}} = 561 \text{ nm}$ )

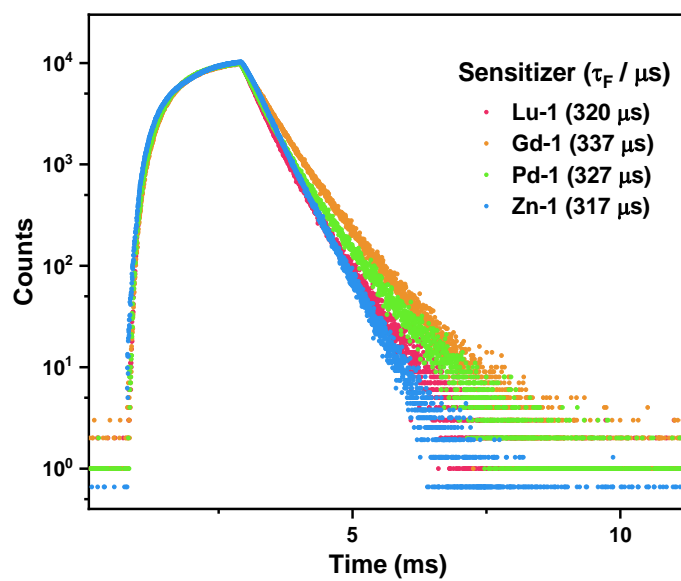


**Fig. S32** Decay spectra of the delayed fluorescence observed in TTA upconversion systems with **Lu-2** and **M-1** ( $M = \text{Gd}, \text{Pd}, \text{Zn}$ ) as sensitizers and BPEA as acceptor in degassed toluene. (Excited by a 561 nm laser,  $\lambda_{\text{em}} = 480 \text{ nm}$ )

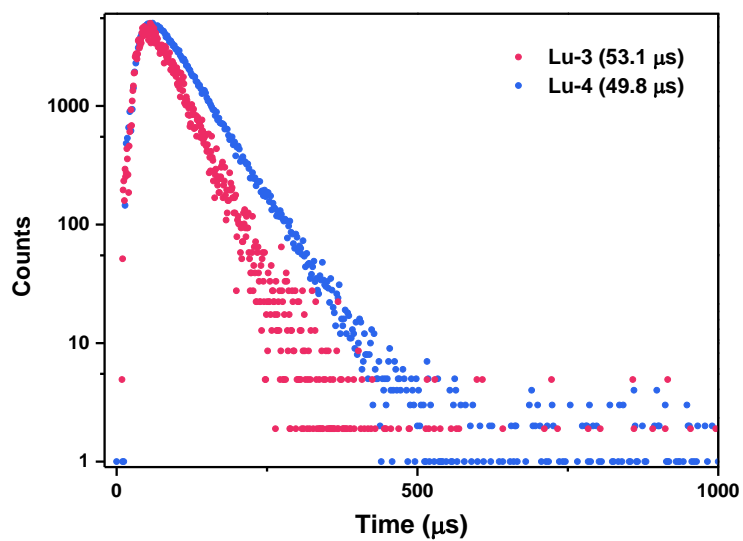


**Fig. S33** Decay spectra of the delayed fluorescence observed in TTA upconversion systems with **Lu-3** and **Lu-4** as sensitizers and rubrene as acceptor in degassed toluene. (Excited by 639 and 659 nm lasers for **Lu-3**/rubrene and **Lu-4**/rubrene systems respectively,  $\lambda_{em} = 561$  nm)

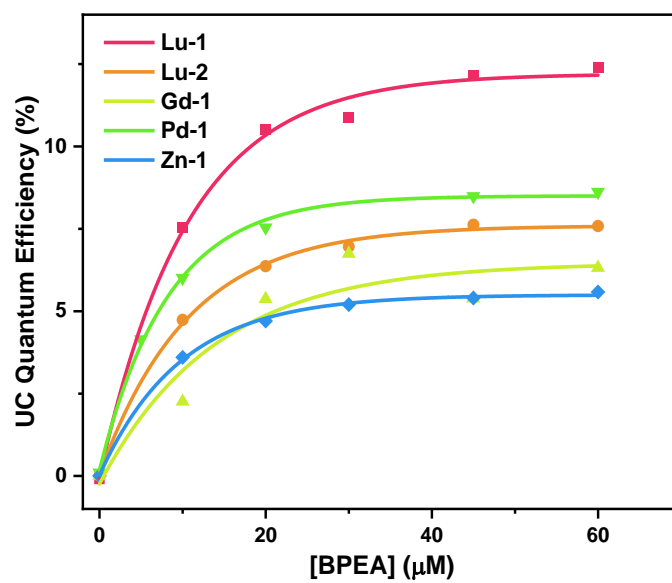


**Fig. S34** Upconversion efficiencies ( $\Phi_{UC}$ ) as a function of BPEA concentration with the sensitizer at fixed concentration (0.5  $\mu\text{M}$ ) in degassed toluene. ( $\lambda_{\text{ex}} = 561 \text{ nm}$ ,  $480 \text{ mW}\cdot\text{cm}^{-2}$ )

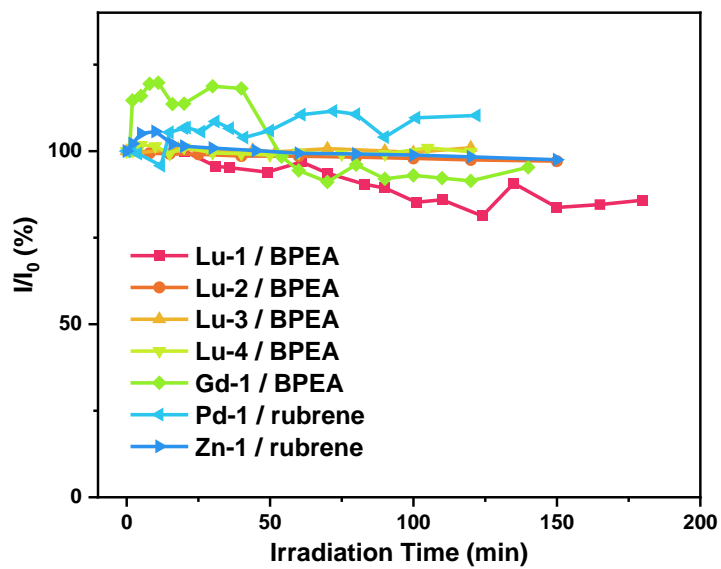


**Fig. S35** Stability of the TTA upconversion emission of different upconversion systems upon continuous irradiation with excitation power density of  $480 \text{ mW}\cdot\text{cm}^{-2}$  in degassed toluene. (Systems with **Lu-3** and **Lu-4** as sensitizers were excited at 639 and 659 nm respectively, while others at 561 nm)

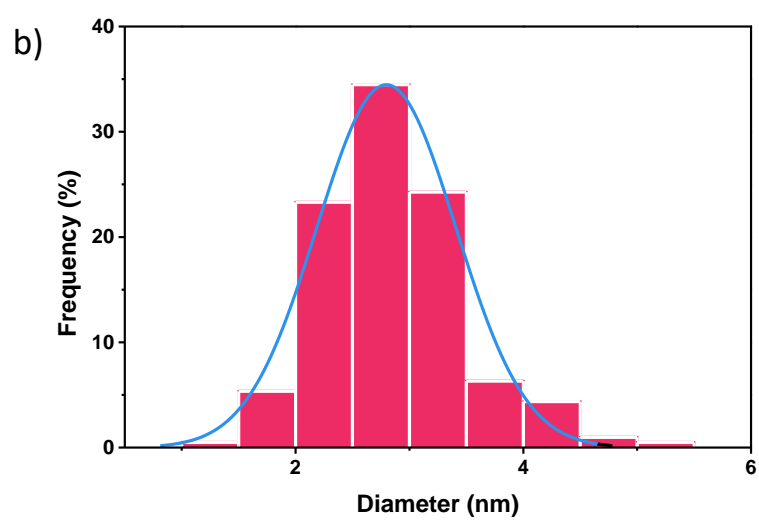
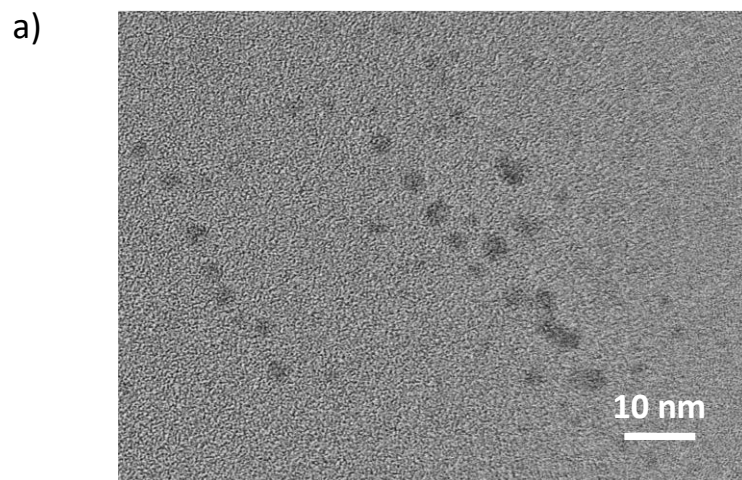


**Fig. S36** (a) Transmission electron microscopy (TEM) image and (b) size distribution of UC-NMs loaded with Lu-2/BPEA at room temperature.

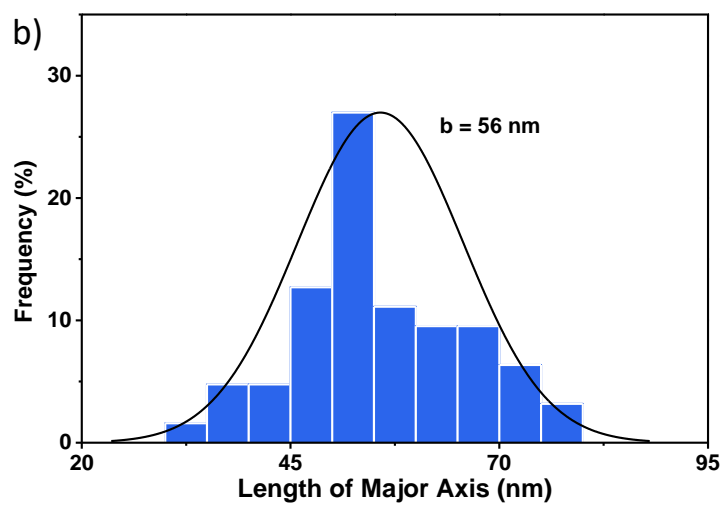
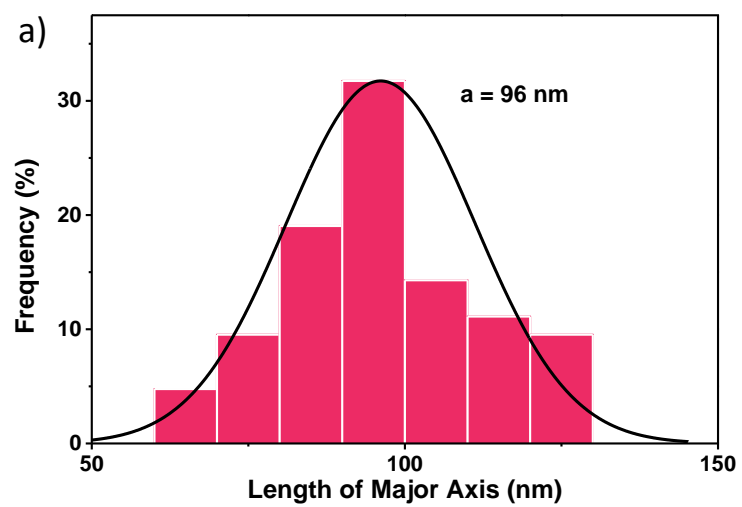


**Fig. S37** (a) Major and (b) minor axis lengths distributions of UC-MSNs loaded with **Lu-1**/BPEA at room temperature measured by TEM.

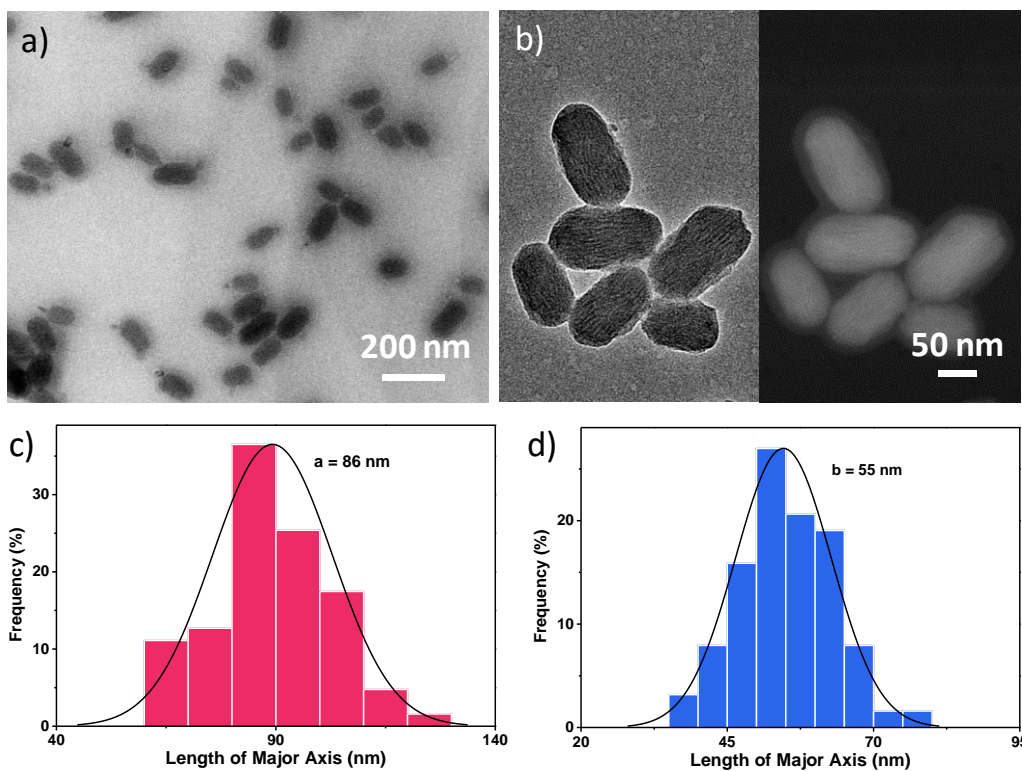


**Fig. S38** (a) Transmission electron microscopy (TEM) image at 25kx magnification, (b) pore channel structure in bright field (left) and dark field (right) TEM image at 60kx magnification, (c) Major axis lengths distribution and (d) minor axis lengths distribution of UC-MSNs loaded with **Lu-2**/BPEA at room temperature.

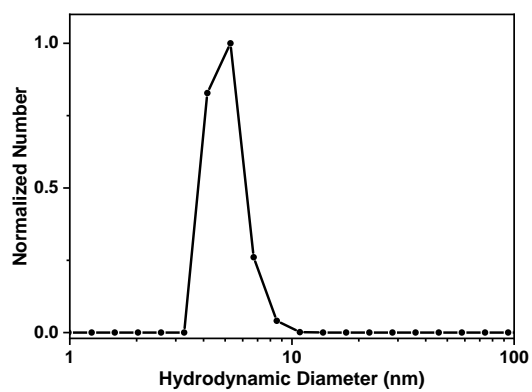


**Fig. S39** Dynamic light scattering (DLS) of **Lu-2/BPEA** loaded UC-NM.

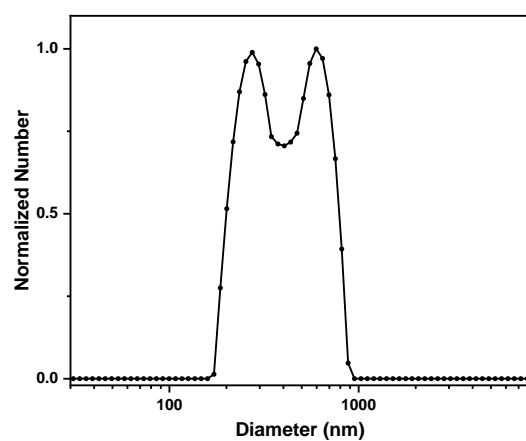


**Fig. S40** Dynamic light scattering (DLS) of Lu-2/BPEA loaded UC-MSN. ( $274\pm 4$  and  $585\pm 8$  nm)

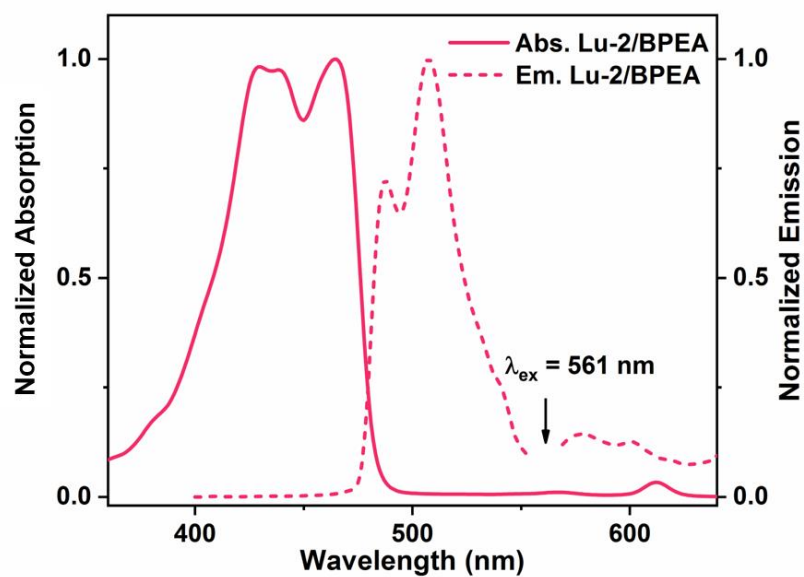


**Fig. S41** Normalized absorption (solid) and emission (dash) spectra ( $\lambda_{ex} = 561 \text{ nm}$ ,  $480 \text{ mW}\cdot\text{cm}^{-2}$ ) of UC-NMs loaded with **Lu-2**/BPEA pair in water under ambient atmosphere.

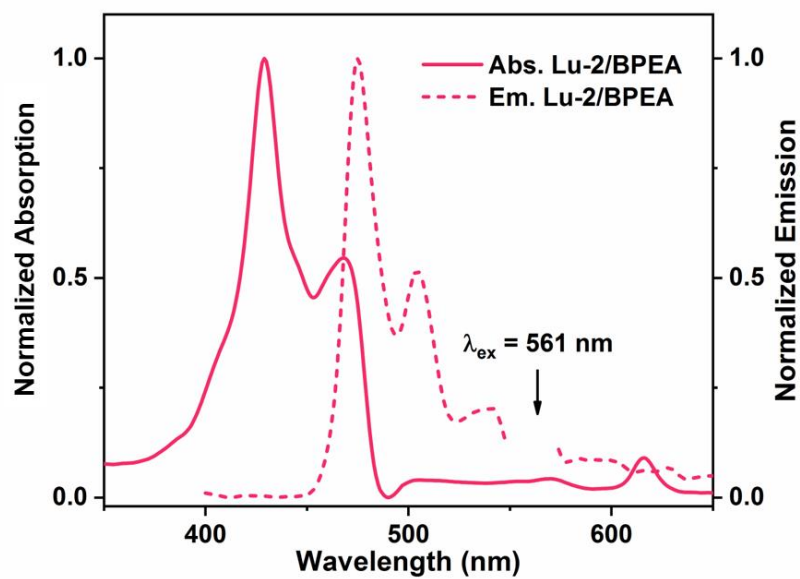


**Fig. S42** Normalized absorption (solid) and emission (dash) spectra ( $\lambda_{ex} = 561 \text{ nm}$ ,  $480 \text{ mW}\cdot\text{cm}^{-2}$ ) of UC-MSNs loaded with **Lu-2**/BPEA pair in water under ambient atmosphere.

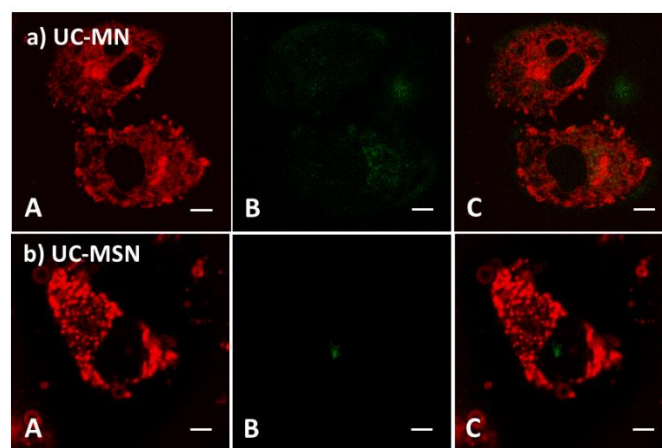


**Fig. S43** Confocal fluorescence image of living HeLa cell with BPEA only (no sensitizer) by 455 - 525 nm channel under laser excitation at (A) 405 nm (red, prompt fluorescence); (B) 543 nm (green, upconverted fluorescence); and (C) merged images of (A) and (B). Row a, b: image of (a) NMs (incubated for 15 min) and (b) MSNs (incubated for 4 h). (Scale bar presents 20  $\mu\text{m}$ )